Performance Analysis of OAM-Based Advanced Symbol Modulation Schemes for OFDM Over FSO System

Athirah Mohd Ramly[1,2], Angela Amphawan[1,2], and Tse-Kian Neo[3(✉)]

[1] Photonics Laboratory, School of Engineering and Technology, Sunway University, 47500 Petaling Jaya, Selangor, Malaysia
[2] Elasticities Research Cluster, Sunway University, 47500 Petaling Jaya, Selangor, Malaysia
[3] Faculty of Creative Multimedia, CAMELOT, Multimedia University, 63100 Cyberjaya, Selangor, Malaysia
tkneo@mmu.edu.my

Abstract. Previous orthogonal frequency division multiplexing over free space optics (OFDM-FSO) systems relied on signal strength, wavelength, and polarisation to multiplex data streams in order to improve signal quality and feasible connection range. Alternatively, this work leverages on orbital angular momentum (OAM) mode division multiplexing with multiple OAM modes (OAM + 1, OAM +2, OAM +3, OAM +4) encountering different modal coupling effects under atmospheric turbulence. Advanced modulation and coding schemes (QPSK, 16QAM, and 64QAM) are deployed to improve the bit-error rate (BER), packet error rate (PER), and achieve a connection range of 1000 m in a free space optical link. OAM +1 was shown to achieve average BER and PER of 10^{-3} at SNR equals to 22 dB and 30 dB respectively.

Keywords: Free space optics · mode division multiplexing · orbital angular momentum · advanced symbol modulation

1 Introduction

Free space optics (FSO) is an attractive contender future networks because it provides a cost-effective solution for high-speed transmission front-haul and backhaul cellular networks and is capable of tackling last-mile bottleneck difficulties [1]. Fast installation and deployment, light-weight equipment, economical equipment and components, license-free transmission, high security, plentiful bandwidth, small beam divergence, and redeploy ability are some of the benefits of FSO over conventional fibre lines and radio frequency (RF) networks [2].

Mode division multiplexing (MDM) have gained significant interest in FSO communications for enhancing transmission capacity [3, 4]. In comparison to other modal bases used in MDM, OAM modes are versatile and may be easily aligned to other optical systems due to their circular symmetry [5]. OAM modes of different topological charges are orthogonal to one another, hence form a basis set of independent channels for

multiple signal transmission [6]. When propagating through a turbulent medium under unfavourable weather conditions, OAM modes are subject to modal coupling, which causes power disparities between OAM modes [7]. This leads to an increase in the bit error rate (BER) at the receiver.

In FSO systems, on-off keying (OOK) modulation is largely used due its simplicity but requires an adaptive threshold on the input power and is susceptible to channel estimation errors [8]. Pulse position modulation (PPM) eliminates the decision threshold dependence and shows good power efficiency [9]. However, this comes with a decline in spectral efficiency. To address the impediments of OOK and PPM, orthogonal frequency division multiplexing (OFDM) is attractive as a multi-carrier modulation scheme using low-speed orthogonal subcarriers [10–12]. Orthogonal frequency-division multiple access (OFDMA) is an OFDM-based multiple access technique in which data is sent to various users on distinct subcarriers. Due to its spectral efficiency and resistance to multipath fading, it is excellent for high data rate transmission in wideband wireless systems [13].

References [14–16] discusses the integration of OFDM and MDM to reduce signal distortion due to turbulence using a variety of spatial modes. Expanding on the previous work, this paper aims to analyse the bit error rate and packet error rate performance of OFDM in conjunction with various advanced symbol modulations and code rates in a FSO system.

The key contribution of this paper is to investigate advanced modulation schemes for OAM-OFDM wireless communication systems, with particular attention on the effect of atmospheric turbulence on both the OAM and OFDM signals. The results obtained are compared with multiple OAM modes such as OAM +1, OAM +2, OAM +3 and OAM +4 in terms of bit error rates (BER) and packet error rates (PER). The influence of different types of coding rates and modulation schemes or also known as modulation and coding schemes (MCS), is investigated as explained in Sect. 2 in this paper. Also, this paper evaluates the throughput of the MCS in terms of free space optics scenarios.

The paper has the following structure. The model system and parameters of the OAM-based advanced modulation schemes for OFDM over FSO description is presented in Sect. 2. The results are analyzed and discussed in Sect. 3. Meanwhile in Sect. 4, it draws the conclusion.

2   Communication Model System and Parameters

First, OFDMA is an OFDM-based multiple access technique in which data is sent to various users on distinct subcarriers. Because of its spectral efficiency and resistance to multipath fading, it is excellent for high data rate transmission in free space optical systems. For these reasons, a simulator was created using the wireless transmission interface protocol regarding the physical (PHY) layer as specified in 3GPP TS 36.201 [17]. The transmitter and receiver block diagrams utilised in this work are shown in Fig. 1.

An electrical signal is generated by an arbitrary waveform generator and advanced symbol modulation schemes and coding rates shown in Table 1. The electrical signal is applied to an intensity modulator (IM) and then indirectly modulated into an optical signal by an 850 nm laser diode.
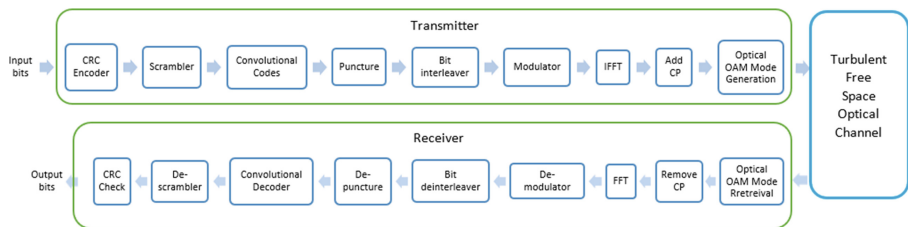
Fig. 1. OFDM-FSO OAM mode division multiplexing system with advanced symbol modulation schemes

Table 1. Modulation and coding scheme used in the simulation

MCS	Type	Code rates	Bit rates, R
1	QPSK	½	8.4 Mbps
2	QPSK	¾	12.6 Mbps
3	16QAM	½	16.8 Mbps
4	16QAM	¾	25.2 Mbps
5	64QAM	½	25.21 Mbps
6	64QAM	¾	37.8 Mbps

The Monte Carlo simulation approach is used to apply PHY channel processing on the OAM FSO channel impulse responses, where BER and PER are calculated an average of 2000 times. The opposite operation of the transmitter is done on the receiver side, along with channel estimation, channel equalisation, and data detection [17].

The cyclic redundancy check (CRC) is used as a verification to identify inadvertent or unintentional data change during the storage or transmission process. CRCs are widely used because they are easy to implement in binary hardware and are particularly excellent at identifying common faults, such as noise in transmission channels. Meanwhile, convolutional codes act as a forward error correction (FEC) code that plays a crucial role in error control in wireless communication.

FEC encoder enables the receiver to identify and repair faults (within certain limits) by inserting some redundant data into the wireless transmission. After encoding, puncturing is the process of removing portions of the parity bits or, in certain cases, systematic codes. The code rate may be readily modified to other coding rates by deleting some of the encoded bits at pre-defined sequences, providing greater precision of coding rates. Bursty errors are common in wireless communication and hence, bit-interleave is implemented to avoid such cases.

Bit interleaving tries to randomise error bursts and imitate random errors for error correction codes. A scrambler is used in a wireless system to remove the lengthy sequence of "0" and "1". This is important because later in the modulation process, the modulator will accept binary bit 0 or 1 as input and output complex-valued modulation signals. This modulation technique is compatible with QPSK, 16QAM, and 64QAM schemes.

A IFFT is implemented in order to reduce the computational complexity for a larger FFT size.

At the receiver, the signals are subjected to an FFT to identify the received frequency domain data symbols that will lead to [13]:

$$y_n = \sum_{m=0}^{N-1} Y_m e^{-j(2\pi nm/N)} n = 0, 1, 2, \ldots, N-1 \qquad (1)$$

A mechanism known as Guard Interval or Cyclic Prefix (CP) is used to avoid inter symbol interference (ISI) and inter carrier interference (ICI) caused by delay spread and transmit/receiver filter group delay. The Cyclic Prefix (CP) is removed by the OFDM demodulator, and a radix-2 FFT (inverse of OFDM signal creation) is conducted on the received base band signal. Frequency selective fading, in conjunction with timing and frequency offset, results in random phase and amplitude change of the constellation on the subcarriers. In an OFDM system, coherent detection is utilised to identify the best feasible limits for the constellation of each subcarrier by utilising estimations of the reference amplitudes and phase.

Six kinds of modulation and coding schemes (MCS) are offered in this simulation, based on [15]. A 20 MHz channel bandwidth is used in this simulation as well as 30 kHz subcarrier spacing. This subcarrier spacing was used for this simulation to accommodate a high delay spread while maintaining a fair cyclic prefix overhead. Whereas the sampling frequency is set to be at 30.72 MHz and the transmission bandwidth is proposed at 18 MHz. The number of FFT size is defined in 2048. The number of OFDM symbol per slot is 7 for normal CP whereas for extended CP, it is set to 6. For normal CP, the CP length is set to 5.2 µs [17].

The modulated optical signals are collimated and linearly polarized, then inserted into tapered waveguides [18] for MDM of OAM +1, OAM +2, OAM +3 and OAM + 4 modes.

The optical signals are transmitted through a free space optical channel of 1000 m. To measure the strength of the atmospheric turbulence, the Rytov variance from intensity profile measurements at the receiver was calculated, to determine the refractive index structure C_n^2 indicating the strength of the atmospheric turbulence [19]. In the experiment, a C_n^2 value in the range of 8 10^{-17} to 4 10^{-16} was obtained, which indicated moderate turbulence.

The OAM modes were obtained using another set of tapered waveguides to reverse the effects of the turbulent channel based on [18]. Modal decomposition based on [20] was performed to obtain the power coupling coefficients of the output OAM modes. The channel impulse responses are measured based on the average refractive index structure.

3   Results and Discussions

Figures 2, 3 and 4 depict the performance of a SISO scenario in wireless radio communication for various MCS modes in free space optics in terms of PER and BER. In the simulation, a perfect channel estimation is employed. Throughout the paper, a packet size of 64 bytes is taken into account. Furthermore, unless otherwise mentioned, each
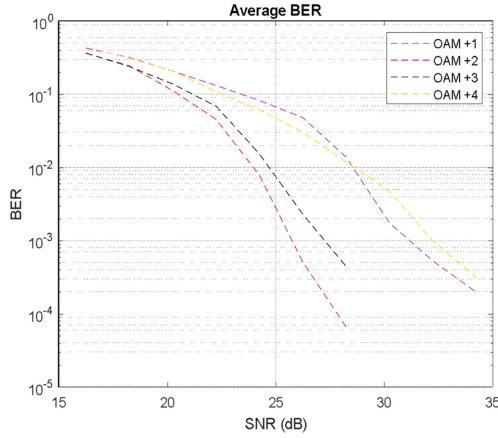
Fig. 2. Bit error rate for OFDM-FSO of different OAM modes OAM +1,OAM +2,OAM +3 and OAM +4

simulation takes into account 2000 samples. A user equipment will be out of service when the SNR falls below 0 dB. A higher SNR value indicates that the signal is clearer. With a lower value, you begin to introduce Gaussian noise (expressed as static), and as the number approaches 1, the static worsens. The noise disrupts your network's signal processing capabilities, resulting in random noise and amplitude modulation. If the SNR value falls below one, the signal is rendered useless. The term for this is the "noise floor". While the UE will be at the maximum MCS at around 24 dB, assuming that a PER transmission objective of 10% is often predicted.

t is also important to note that MCS 4, i.e., 16QAM ¾ coding rate, is rendered obsolete for these channel circumstances since it is surpassed by 64QAM ½ coding rate over the entire SNR range while providing the same nominal data rate. Unless otherwise mentioned, the ideal channel estimation technique is adopted throughout the study for consistency and comparability. Figures 2 and 3 illustrate the average bit-error rate (BER) and packet error rate (PER) of the various MCS schemes for FSO. Different values of OAM which is OAM +1, OAM +2, OAM +3 and lastly, OAM +4 is plotted in Fig. 1. It is shown that OAM +1 has the best average BER, and PER which are 22 dB SNR at BER = 10^{-3} and 30 dB at PER = 10^{-3}.

Figure 4 depicts the average attainable throughput for the MCS modes in the free space optics scenario based on OAM +1. The feasible throughput is calculated by multiplying the data rate by the residual packet error rate and is thus measured in bits per second. The following equations approximate the link throughput:

$$Throughput \approx R(1 - PER_{phy}) \quad\quad (2)$$

where R and PER denote the bit rate and residual packet error rate for a given mode. The throughput envelope is calculated by employing ideal adaptive modulation and coding (AMC) based on the (throughput) optimal switching point. Given a system bandwidth of 20 MHz, maximum throughput can be obtained in a SISO situation with an average SNR of 27 dB.
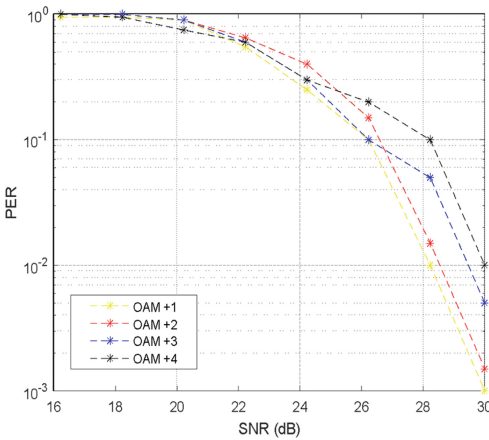
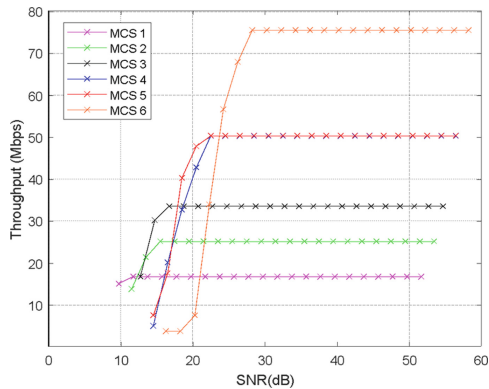**Fig. 3.** Packet error rates for OFDM-FSO of different OAM modes OAM +1, OAM +2, OAM +3 and OAM +4

Fig. 4. Average throughput for different modulation and coding schemes based on OAM +1

4   Conclusion

The suggested approach, OFDM-FSO, generated outcomes in terms of BER, PER, and throughput by merging OAM modes with modulation and coding schemes. An electrical signal is delivered to an intensity modulator (IM), which is then converted indirectly into an optical signal by an 850 nm laser diode. The signal is collimated and linearly polarised before being introduced into tapered waveguides to produce OAM +1, OAM +2, OAM +3, and OAM +4 modes. The OAM modes are sent across a 1000-m free space optical connection, and the channel impulse responses are monitored. The OAM +1 was shown to achieve average BER and PER of 10^{-3} at SNR equals to 22 dB and 30 dB respectively.

Authors' Contributions.   All authors conceived and designed the study. All authors conducted the experiment, analysed the data, and wrote the paper.

References

1. A. Jahid, M. H. Alsharif, and T. J. Hall, "A contemporary survey on free space optical communication: Potentials, technical challenges, recent advances and research direction," *Journal of Network and Computer Applications,* vol. 200, p. 103311, 2022/04/01/ 2022.

2. H. Kaushal and G. Kaddoum, "Optical Communication in Space: Challenges and Mitigation Techniques," *IEEE Communications Surveys & Tutorials,* vol. 19, no. 1, pp. 57–96, 2017.

3. J. Zhou, J. Wu, J. Zong, and Q. Hu, "Optimal Mode Set Selection for Free Space Optical Communications in the Presence of Atmosphere Turbulence," *Journal of Lightwave Technology,* vol. 36, no. 11, pp. 2222–2229, 2018.

4. A. Trichili, K. H. Park, M. Zghal, B. S. Ooi, and M. S. Alouini, "Communicating Using Spatial Mode Multiplexing: Potentials, Challenges, and Perspectives," *IEEE Communications Surveys & Tutorials,* vol. 21, no. 4, pp. 3175–3203, 2019.

5. M. Ma, Y. Lian, Y. Wang, and Z. Lu, "Generation, Transmission and Application of Orbital Angular Momentum in Optical Fiber: A Review," (in English), Review vol. 9, 2021-November-29 2021.

6. A. E. Willner *et al.*, "High-capacity Free-space Optical Communications Using Multiplexing of Multiple OAM Beams," in *Electromagnetic Vortices*, 2021, pp. 357–400.

7. A. E. Willner *et al.*, "Chapter 10 - Causes and mitigation of modal crosstalk in OAM multiplexed optical communication links," in *Structured Light for Optical Communication*, M. D. Al-Amri, D. L. Andrews, and M. Babiker, Eds.: Elsevier, 2021, pp. 259–289.

8. W.-H. Shin, H.-J. Park, and S.-K. Han, "Periodic Adaptive Threshold Estimating Method for Free Space Optical Communication," in *Asia Communications and Photonics Conference*, Guangzhou, Guangdong, 2017, p. Su2A.58: Optica Publishing Group.

9. H. Fu, P. Wang, T. Liu, T. Cao, L. Guo, and J. Qin, "Performance analysis of a PPM-FSO communication system with an avalanche photodiode receiver over atmospheric turbulence channels with aperture averaging," *Applied Optics,* vol. 56, no. 23, pp. 6432–6439, 2017/08/10 2017.

10. M. Singh, S. Chebaane, S. Ben Khalifa, A. Grover, S. Dewra, and M. Angurala, "Performance Evaluation of a 4×20-Gbps OFDM-Based FSO Link Incorporating Hybrid W-MDM Techniques," (in English), Original Research vol. 9, 2021-September-20 2021.

11. J. Zhou, Y. Shao, Z. Wang, C. Li, Y. Zhou, and W. Ma, "A 16PSK-OFDM-FSO Communication System under Complex Weather Conditions," *Optics and Photonics Journal,* vol. 6, pp. 131–135, 2016.

12. S. Chaudhary, A. Amphawan, and K. Nisar, "Realization of free space optics with OFDM under atmospheric turbulence," *Optik - Int. Journal for Light and Electron Optics,* vol. 125, no. 18, pp. 5196–5198, September 2014 2014.

13. R. v. Nee and R. Prasad, *OFDM for Wireless Multimedia Communications*. Artech House, Inc., 2000.

14. E. M. Amhoud, M. Chafii, A. Nimr, and G. Fettweis, "OFDM with Index Modulation in Orbital Angular Momentum Multiplexed Free Space Optical Links," in *2021 IEEE 93rd Vehicular Technology Conference (VTC2021-Spring)*, 2021, pp. 1–5.

15. A. Amphawan, S. Chaudhary, and B. B. Gupta, "Secure MDM-OFDM-Ro-FSO System Using HG Modes," *International Journal of Sensors Wireless Communications and Control,* vol. 5, no. 1, pp. 13–18, 2015.

16. A. Amphawan, S. Chaudhary, and V. W. S. Chan, *2 x 20 Gbps - 40 GHz OFDM Ro-FSO transmission with mode division multiplexing* (2014). 2014.
17. "(E-UTRA) and (EUTRAN): Physical Channels and Modulation," Technical Specification Group Radio Access Network2008, Available: http://www.3gpp.org/ftp/Specs/html-info/36211.htm.
18. N. A. Mahadzir *et al.*, "Tapered waveguide design for mode conversion in mode division multiplexing (MDM)," *Electromagnetics,* vol. 41, no. 6, pp. 448–458, 2021/08/18 2021.
19. A. Amphawan, N. Arsad, T.-K. Neo, M.B. Jasser, "Post-Flood UAV-Based Free Space Optics Recovery Communications with Spatial Mode Diversity". *Electronics* **2022**, 11, x.
20. A. Amphawan and D. O'Brien, "Modal decomposition of output field for holographic mode field generation in a multimode fiber channel," *International Conference On Photonics 2010*, 2010, pp. 1–5, https://doi.org/10.1109/ICP.2010.5604377.